

# Giant sheath-folded nappe stack demonstrates extreme subhorizontal shear strain in an Archean orogen

Yating Zhong<sup>1</sup>, Timothy M. Kusky<sup>1,2\*</sup> and Lu Wang<sup>1</sup>

<sup>1</sup>State Key Laboratory of Geological Processes and Mineral Resources, and Center for Global Tectonics, School of Earth Sciences, China University of Geosciences, Wuhan 430074, China

<sup>2</sup>Badong National Observation and Research Station of Geohazards, China University of Geosciences, Wuhan 430074, China

## ABSTRACT

Giant sheath-folded nappes are associated with suture zones and emplacement of far-traveled allochthons in Phanerozoic orogens, demonstrating a rare but significant geologic phenomenon indicative of modern-style plate tectonics. We document the world's oldest-known subhorizontal mega-scale sheath fold from Archean Alpine-style nappes of the Central orogenic belt, North China craton. The Zhanhuang nappes are recumbent Alpine-style forearc-affinity metabasaltic and metasedimentary nappes emplaced over a passive continental margin in the Archean, marking an ancient suture zone. Field evidence shows multiscale sheath folds from decimeters to tens of meters in size, and our three-dimensional fence profile, fold hinges, kinematic lineations, and lithological traces define an ~1-km-long (parallel to the *x*-axis) sheath fold in the core of the nappe stack. Structural analysis statistically demonstrates the macro-scale recumbent sheath-folded nappe preserves a complete 180° hinge-line curvature. The giant sheath fold plunges northwest, reflecting its formation during non-coaxial, top-to-the-southeast shearing with extremely high shear strain ( $\gamma \geq 10$ ), equated to >10 km of ductile slip on the bounding surfaces. Slip vectors derived from S-C fabrics on overturned limbs are consistent with rotation into the southeast-directed transport direction, parallel to the similarly rotated fold hinges. Comparison of the giant sheath-folded nappes from the Archean Zhanhuang example with mega-scale sheath folds in Phanerozoic and Proterozoic orogens shows that Neoproterozoic lithosphere was stiff enough to allow tectonics to operate in a manner analogous to modern-style plate tectonics.

## INTRODUCTION

There has been a long-lasting debate on the early Earth's tectonic regime and how long the modern plate-tectonic mode has been in operation (Lenardic, 2018; National Academies of Sciences, Engineering, and Medicine, 2020; Sun et al., 2021). The rarity of diagnostic hallmark features of modern plate tectonics identified in Precambrian basement inevitably hinders reaching geological consensus on whether or not plate tectonics operated on early Earth (e.g., Weller and St-Onge, 2017; Lenardic, 2018; Korenaga, 2021). Giant (mountain-scale) recumbent sheath folds represent a rare geologic phenomenon known to be associated with emplacement of some large allochthonous thrust nappes in Phanerozoic orogens, including

beneath the Semail ophiolite (Oman), in several European Alpine examples, and in the Neoproterozoic Lapland-Kola orogen (Baltic Shield) (Cornish and Searle, 2017; Warren et al., 2003; Mudruk et al., 2013). All are associated with suture zones and the emplacement of distant, generally forearc nappes over passive-margin sequences and exhibit large horizontal strain associated with plate-tectonic displacements (Table S1 in the Supplemental Material<sup>1</sup>). We document a pile of kilometer-scale subhorizontal sheath-folded nappes in an Archean orogen and compare it with other well-established large sheath folds globally in orogens of all ages. Large-scale recumbent sheath folds are diagnostic of long-distance (plate tectonic) lateral displacement, and we demonstrate that the same large-scale subhorizontal shear strain and displacements are preserved in Phanerozoic,

Proterozoic, and, based on our study, Archean orogens, hinting that those similar structures may have formed by similar processes, under similar conditions, throughout geologic time. Our results are compatible with other evidence for large subhorizontal thrusts, nappes, and displacements in the Archean, especially well documented from Greenland and the Pilbara craton (Western Australia) (e.g., Hanmer and Greene, 2002; Nutman et al., 2020; Kusky et al., 2021b), but this is the first example of a subhorizontal mega-scale sheath-folded nappe pile known from the Archean, adding one more feature of modern-style tectonics to the Archean record.

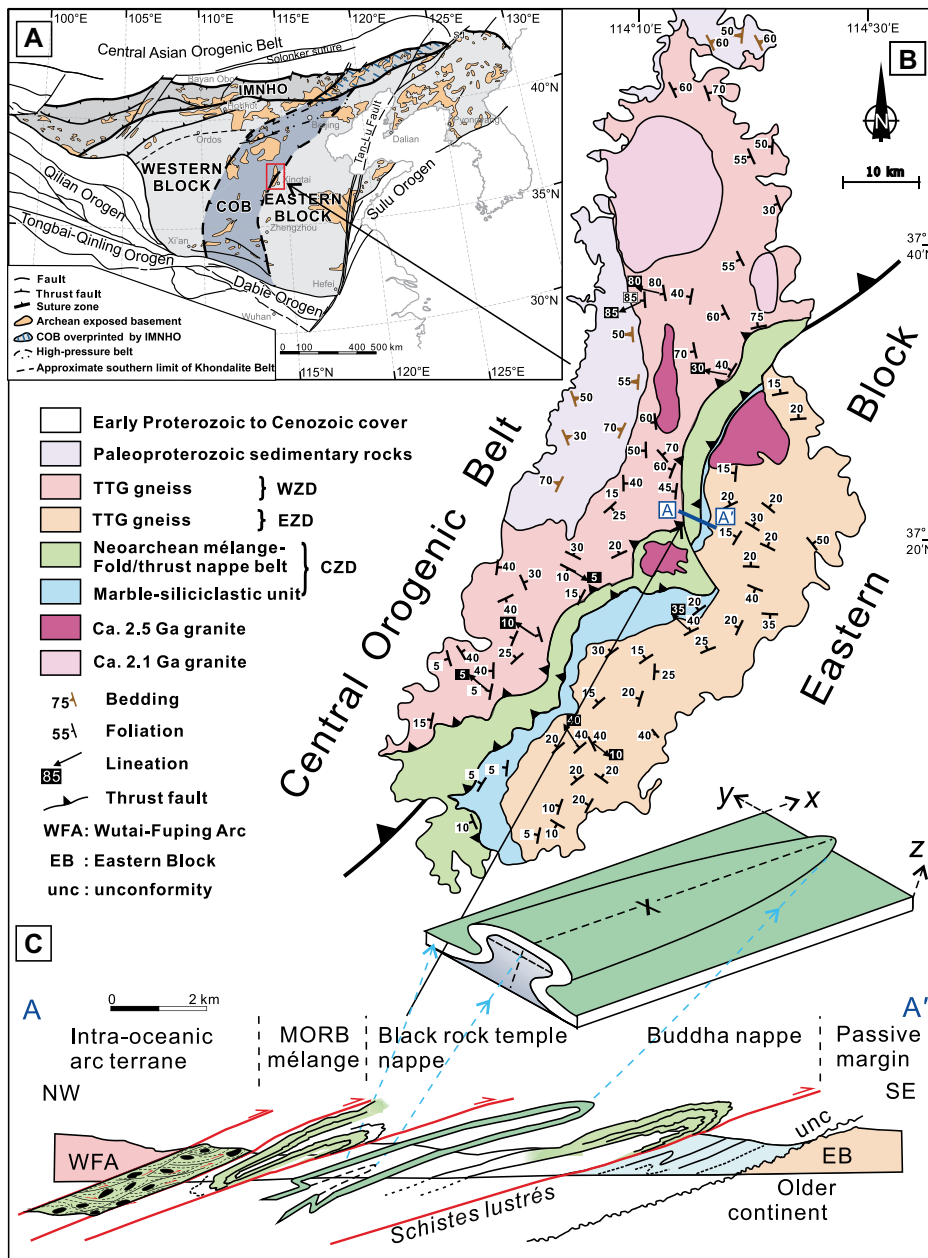
## GEOLOGICAL SETTING

The Archean Zhanhuang nappe stack in northern China is one of the most ancient, well-preserved, Alpine-style subhorizontal fold-thrust nappe belts known (Zhong et al., 2021), although remnants or traces of similar orogenic structures have been reported (e.g., Windley et al., 2021). It is situated at the front (foreland) of the Central orogenic belt in the North China craton. The Central orogenic belt is an ~1600-km-long, nearly north-south-trending Neoproterozoic orogen (Fig. 1A) formed during convergence and collision between an intra-oceanic arc terrane in the west and the ancient continental Eastern block in the east (Kusky et al., 2016, 2020; Wang et al., 2017). The Neoproterozoic Central orogenic belt exhibits a well-defined tectonic zonation comparable with classical Phanerozoic orogenic belts (e.g., the Cenozoic Austro-Alpine orogen), grading from hinterlands of strongly deformed intra-oceanic arc magmatic rocks through zones of ca. 2.5 Ga ophiolitic-tectonic mélange with local paired metamorphic, high-pressure and ultrahigh-pressure assemblages (Kusky et al.,

\*E-mail: [tkusky@gmail.com](mailto:tkusky@gmail.com)

<sup>1</sup>Supplemental Material. Table S1 (global examples of subhorizontal mega-scale sheath folds). Please visit <https://doi.org/10.1130/G49599.1> to access the supplemental material, and contact [editing@geosociety.org](mailto:editing@geosociety.org) with any questions.

CITATION: Zhong, Y., Kusky, T.M., and Wang, L., 2022. Giant sheath-folded nappe stack demonstrates extreme subhorizontal shear strain in an Archean orogen: *Geology*, v. XX, p. , <https://doi.org/10.1130/G49599.1>



2018; Wang et al., 2019; Huang et al., 2020; Kusky et al., 2020, 2021a) to a 15–20-km-wide belt of ductile fold nappes and thrusts with forearc-affinity assemblages (Zhong et al., 2021) and eventually into a relatively undeformed 2.5 Ga foreland basin now preserved as several relict sequences including the Qinglong and Songshan sequences (2.50–2.45 Ga) (Kusky et al., 2016; Huang et al., 2019). The foreland basin deposits locally overlie passive-margin sediments and the unconformably underlying

crystalline basement of the Eastern block of the North China craton (Kusky et al., 2016).

The Archean Alpine-style allochthons form a pile of recumbent fold nappes bearing a classical forearc subduction-initiation sequence (ca. 2.7 Ga mid-oceanic ridge basalt, picritic-boninitic and island-arc tholeiitic basalt) that glided along highly sheared thrust zones to be emplaced over a Neoproterozoic passive-continental-margin sequence at ca. 2.52 Ga (Zhong et al., 2021). The location of the nappe pile marks

the suture zone between the Wutai-Fuping arc and Eastern block continent. Rocks within the suture zone are dominated by intense southeast-directed subhorizontal thrust-sense shear evidenced by the ubiquity of structures including rotated porphyroclasts and/or blasts, S-C fabrics, asymmetric folds and duplex structures, and consistent regional northwest-plunging mineral lineations and southeast fold vergence (Figs. 1C and 2A). The folds are non-cylindrical, extremely tight to isoclinal structures, indicating high strain. The associated deformation is interpreted to have been developed at ca. 2.50 Ga, constrained by (1) geological crosscutting relationships (Wang et al., 2013), and (2) maximum depositional ages from the Alpine-style *schistes lustrés* unit underlying the fold-nappe stack (Zhong et al., 2021).

### GEOMETRY OF A MOUNTAIN-SCALE ARCHEAN SHEATH FOLD

Sheath folds are non-cylindrical cone-shaped structures, characterized by highly curvilinear fold hinges ( $>90^\circ$ ) with parabolic noses and closed layers revealed by elliptical cross sections (eye structures) when viewed perpendicular to the shearing direction (Cobbold and Quinquis, 1980; Alsop and Holdsworth, 2004, 2006; Adamuszek and Dabrowski, 2017). Our detailed structural mapping reveals that mesoscopic elliptical folds are commonly exposed in the mechanically layered Zhanhuang fold nappe–thrust belt (Fig. 2A). Tongue-like morphologies with apical angles of  $\sim 30^\circ$ , identified on the XY planes of decimeter-scale sheath folds, together with fold hinge lines systematically varying and rotating toward major culminations (Figs. 2B, 2C, and 2D) display the curvilinearity of fold hinges accentuated toward the stretching direction (Fig. 2E). The hinge lines show a  $180^\circ$  rotation from northeast-southwest (orogen parallel) to southeast, parallel to the stretching direction (Fig. 2F).

Macroscopic elliptical folds are shown by cascading fold limbs wrapping around eye-type sheath folds (Fig. 2G) whose fold asymmetry (S- and Z-shaped on opposing fold limbs) viewed on YZ surfaces varies systematically, together with reversals in facing associated with the relative position of culminations and/or depressions on the enveloping sheath fold (Figs. 2G and 2H). This geometry of the large-scale sheath structure is corroborated by the lower-hemisphere projection of hinge lines measured along the entire fold nappe–thrust belt, which define a well-developed fold hinge girdle with  $180^\circ$  of hinge-line curvature, plunging northwest, depicting a regional-scale sheath geometry formed by extremely high shear strain in the mechanically stratified sequence (cf. Dell’Ertola and Schellart, 2013) (Fig. 2F) with a top-to-the-southeast shear sense.

Figure 3 is a three-dimensional fence profile based on detailed mapping and analysis of

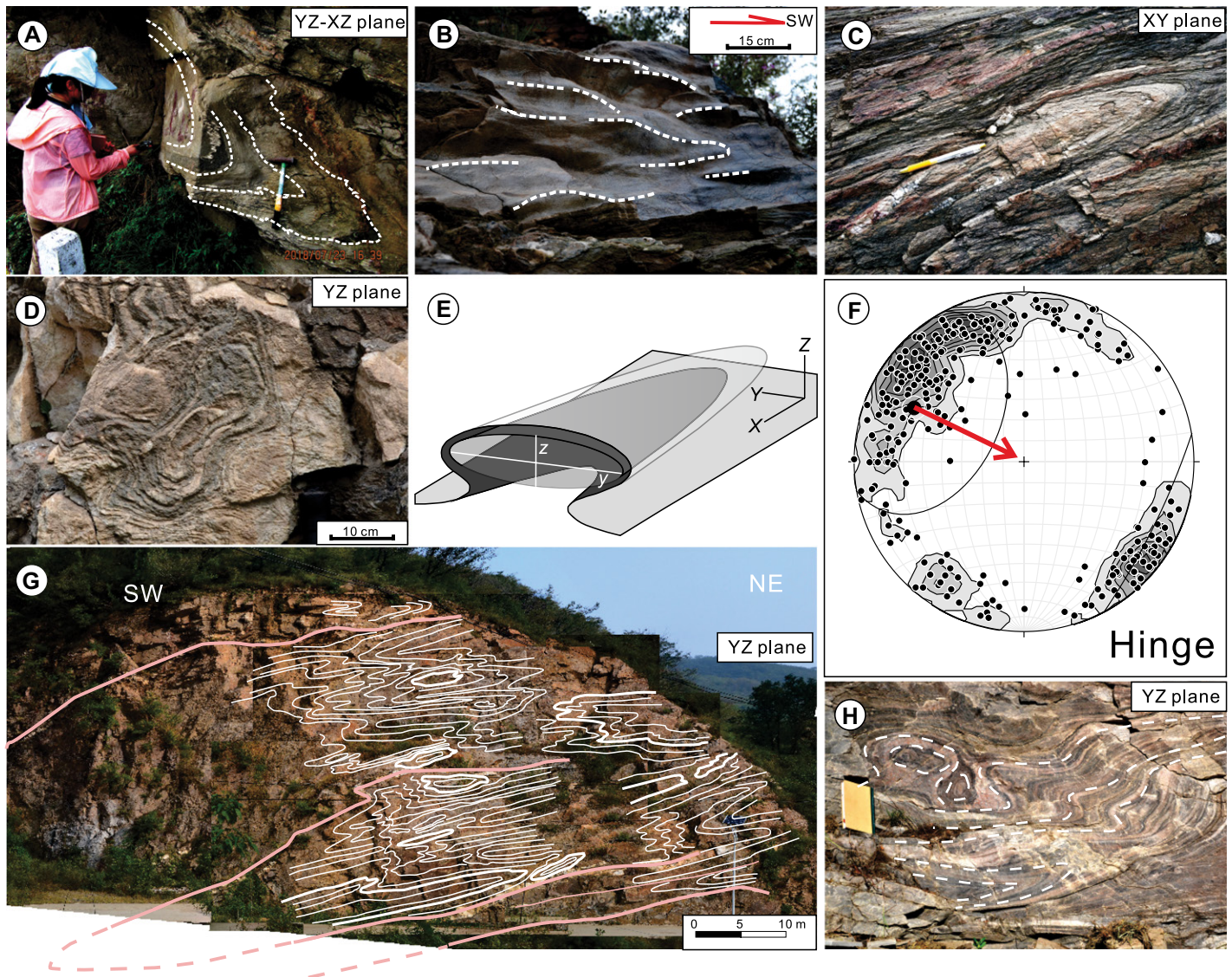


**Figure 2.** Field photos illustrating views of sheath folds at various scales (Zanhuang nappe stack in northern China). (A) Three-dimensional perspective illustrating conical sheath form. (B) Sheath-fold surface displaying curvilinearity of fold hinges. (C) Curvilinear folds, which are convex up when viewed in inclined (XY plane) axial surface. (D) Elliptical “eye-type” shape exposed perpendicular to the long axis of sheath folds. (E) Three-dimensional model and corresponding geometric orientation in (X-Y-Z) coordinate of simple sheath folds. (F) Equal-area plot of fold hinge lines (1% area contour interval) showing a great-circle girdle with 180° of hinge line curvature; large black point represents sheath fold axis about a conical best fit, and red arrow shows transport direction. (G) Transport-normal photograph offering a view of an elliptical fold indicative of a macroscopic sheath fold form marked by white lines; pink lines represent folded quartz vein forming isoclinal recumbent folds wrapping around those sheaths (photo looking northwest, outcrop strike 65°). (H) Fold asymmetry viewed on surfaces perpendicular to the x-axis varies systematically, corresponding to discrete fold limbs from a distinct elliptical sheath fold;  $\Omega$ -shaped sheath fold is shown at top left corner above a notebook (36 cm long).

profiles cutting through the giant sheath fold sequence in various orientations, allowing unique views into the heart of the structure. This technique shows that the structure consists of at least three stacked sheath folds within the larger sheath structure. The ellipsoidal sections are preserved at high angles to the x-axis of the sheath fold as shown in Figures 3A and 3B, while recumbent isoclinal anticlines stacked upon one another are exposed subparallel to the x-axis as shown in Figure 3D. The doubly verging geometries illustrated on the profiles nearly orthogonal to each other show typical

sheath-fold forms, explaining the opposite vergence shown in Figures 3D and 3E. Therefore, the large-scale sheath fold extending for a distance of  $\sim 1$  km across strike provides a minimum estimate for the length of the (southeast stretching) x-axis of the macroscale sheath fold (Fig. 3). Based on comprehensive regional-scale structural analysis, the geometrical similarity between individual and domain-scale sheath folds and mesoscopic- and macroscopic-scale sheath folds implies that sheath folding is common at all scales in the fold nappe–thrust belt and the giant sheath fold mapped here is perhaps

just the core of an even larger structure including the entire fold nappe–thrust stack (Fig. 1C).

The regional fold nappes are tight to isoclinal and recumbent with highly attenuated overturned limbs, which typically display S-C fabrics. The sense of shearing, inferred by the S-C fabrics on the reversed limbs of recumbent nappes, shows rotational axes that differ on either side of the main direction of shearing, corresponding to the strain gradient, or strain-rate gradient, during sheath folding and high-strain shearing, with the main transport direction bisecting the curved arc of the S-C intersection lineations (Fig. 4).

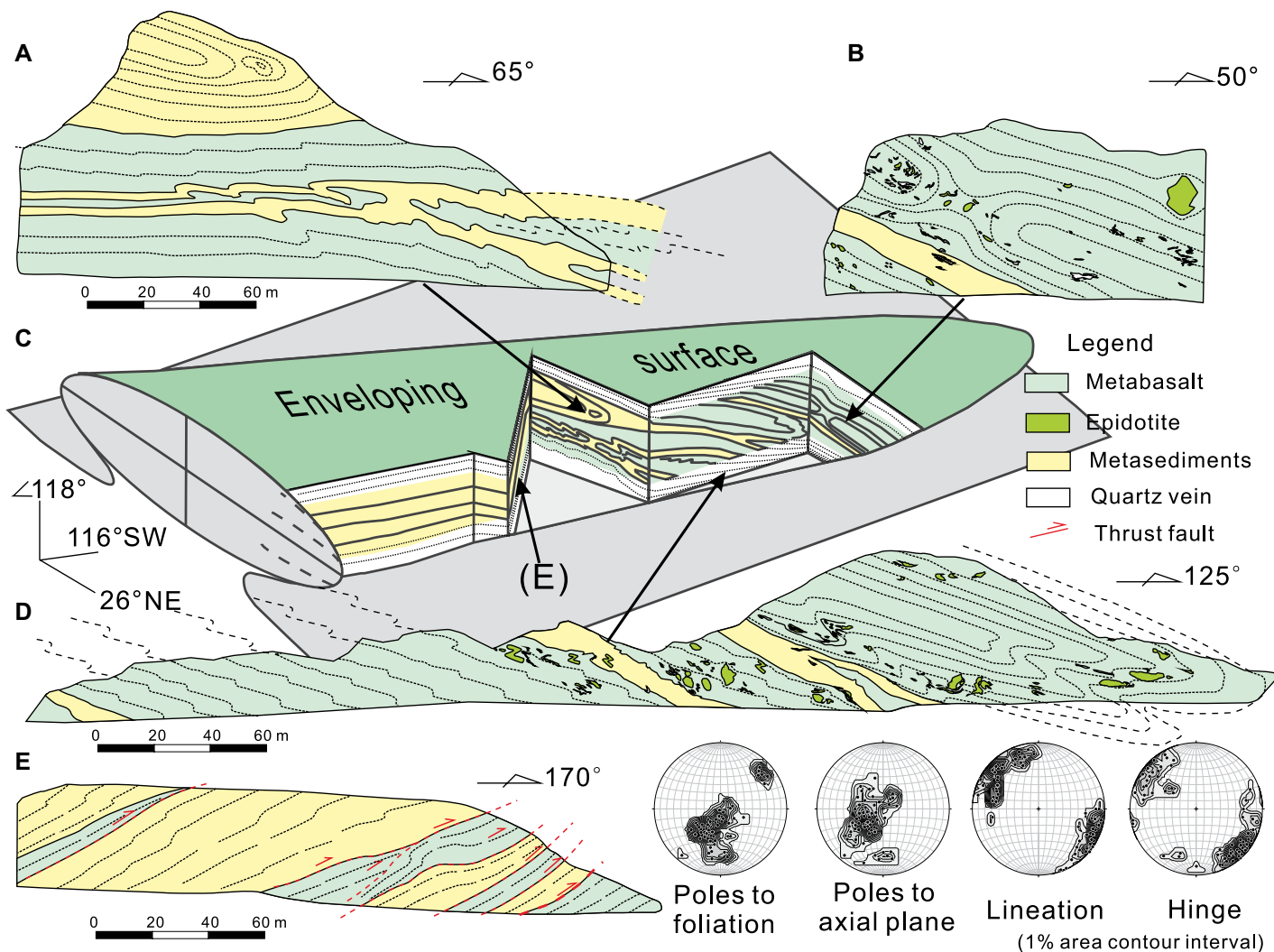


**Figure 3.** Fence profile cut through a sheath fold sequence in various orientations allowing unique views into the heart of the structure.

Progressive nappe propagation under top-to-the-southeast simple and/or general shear initially led to tight to isoclinal, recumbent fold forms and extreme thinning of rotated overturned limbs of the pile of recumbent folds. Continuous high shear strain further resulted in the base of non-cylindrical sheath folds forming recumbent fold nappes at advanced stages and high shear strain ( $\gamma \geq 10$ ). Consequently, the convex-up culmination surface coupled with an antiformal closure is present (Figure 2 showing the real outcrop data, and Figure 4 as a schematic model), on which mineral lineations became discordant with the rotated fold hinges during noncylindrical folding, while the majority formed parallel to the fold axis ( $x$ -axis). This is indicative of intensive rotation of fold hinges toward the mineral lineation that initiated at a high angle to shear during progressive non-coaxial deformation, and ended up with parallel hinges and mineral lineations (Fig. 4). Slip vectors, determined by the direction on the C-planes oriented  $90^\circ$  from the intersections between S-planes and C-planes, are rotated correspondingly, indicating

that the entire nappe system slipped parallel to the fold axis while others slipped clockwise or anticlockwise on either side of the main direction of shearing.

#### TECTONIC SIGNIFICANCE

Sheath folds are associated with shear zones and indicate exceptionally high strain. They are typically considered to be developed by the rotation of fold hinges toward the transport direction during progressive non-coaxial deformation (Cobbold and Quinquis, 1980; Lacassin and Mattauer, 1985; Carreras et al., 2005; Alsop and Holdsworth, 2006; Dell'Ertale and Schellart, 2013; Adamuszek and Dabrowski, 2017; Maino et al., 2021). Given that large shear strain ( $\gamma \geq 10$ ) is required by the simple shear mechanism, the development of a subhorizontal kilometer-scale sheath fold corresponds to no less than 10 km of subhorizontal displacement in this Archean orogen. This does not account for additional displacements along thin shear zones, which are significant (Zhong et al., 2021).

Giant kilometer-scale sheath folds are rare and mainly reported from high-shear-strain zones in orogenic belts. By compiling case studies of well-known large-scale sheath folds worldwide (Table S1), we show that kilometer-scale sheath folding coincides with collisional processes in a horizontal compressional regime during orogeny, and all known occurrences of large-scale sheath folds are tectonically situated in suture zones marking places where two, once widely separated tectonic blocks (arcs, continents, plateaus, upper-plate ophiolites, etc.) have collided, with the sheath folds forming along the boundaries (sutures) between the different terranes (Cornish and Searle, 2017; Searle and Alsop, 2007; Lacassin and Mattauer, 1985; Seno et al., 1998; Maino et al., 2015; Bonamici et al., 2011; Mudruk et al., 2013). Documentation of large-scale subhorizontal sheath folds essentially demonstrates a long-distance tectonic transport of the allochthonous unit. The case studies (Table S1) verify that other kilometer-scale sheath-fold structures have been documented in younger orogens of all ages, from

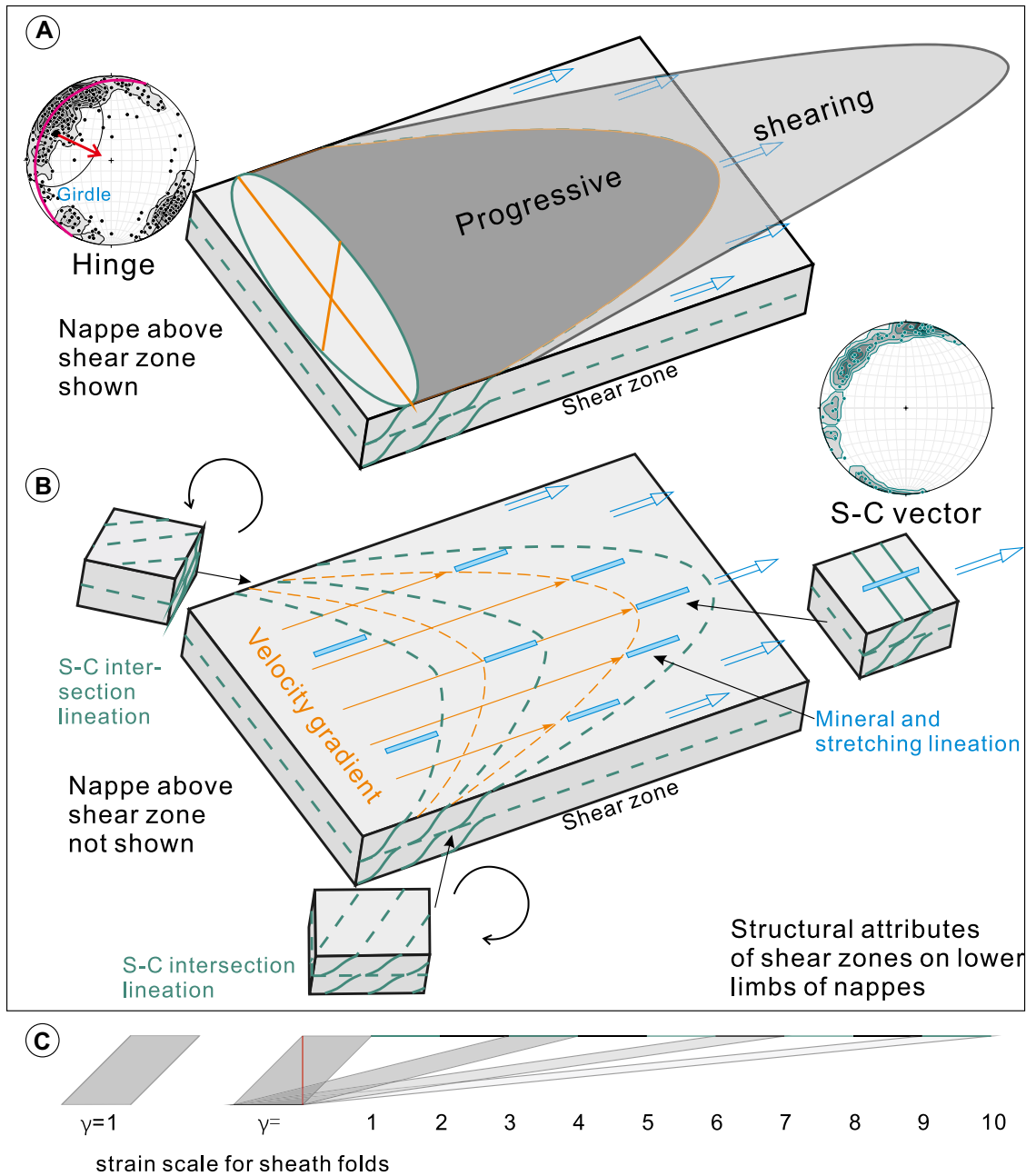


**Figure 4.** (A,B) Diagrams illustrating the geometric elements of sheath folding during progressive high-strain shearing of the Zhanhuang fold nappe stack (north China craton). Velocity gradient is marked by the curvilinearity of hinge rotation toward the transport direction (A). S-C intersection lineation (B) is curved, corresponding to the process of sheath folding, illustrated by the equal-area plot of the S-C vector, which is the direction perpendicular to the intersections between S- and C-planes on the C-planes, which are rotated systematically about the transport direction (stereonet in B with 1% area contour interval). (C) Strain ( $\gamma$ ) from 1 to 10, graphically illustrating that because sheath folds form at  $\gamma \geq 10$  and the sheath fold is  $\sim 1$  km in scale, structures record subhorizontal displacement of  $\geq 10$  km in this zone of the Zhanhuang thrust nappe stack.

the Phanerozoic, the Proterozoic, and, with this discovery, now the Archean. It is therefore suggested that crustal-scale lateral motions can be documented back to the Archean and provide positive evidence for the operation of horizontal plate motions in the ancient Earth.

This is the oldest-known giant recumbent sheath-folded nappe in the world that explicitly demonstrates extreme subhorizontal shear strain. The structural style and kinematic evolution restored in this contribution dramatically differ from those suggested in the Archean hot-orogen model (Chardon et al., 2009) by the presence of (1) strain localization along large-scale thrusts in a convergent setting, (2) lateral variation in metamorphic grade, and (3) reversal of structural and stratigraphic successions

(Zhong et al., 2021). Additionally, a remarkable long distance ( $>3500$  km) of relative displacement between the arc and continent has been proposed (Zhong et al., 2021). Combined with identification of paired metamorphism in the North China craton (Huang et al., 2020) and of seismic reflection of relict slabs in the Slave and Superior cratons (Canada) (Percival et al., 2012), the evidence for the operation of ancient plate tectonics is compelling.

#### ACKNOWLEDGMENTS

This work was supported by the National Natural Science Foundation of China (grants 41890834, 91755213, 41961144020, 41602234, 41888101), Chinese Ministry of Education (grant BP0719022), the Chinese Academy of Sciences (grant QYZDYS-SWDQC017), the Chinese Ministry of Education

(grant BP0719022), and the MOST Special Fund (MSF-GPMR02-3) of the State Key Laboratory of Geological Processes and Mineral Resources, China University of Geosciences (Wuhan). We thank Ross Mitchell, Wenjiao Xiao, and an anonymous reviewer for helpful comments that improved the paper.

#### REFERENCES CITED

- Adamuszek, M., and Dabrowski, M., 2017, Sheath folds as a strain gauge in simple shear: *Journal of Structural Geology*, v. 102, p. 21–36, <https://doi.org/10.1016/j.jsg.2017.06.008>.
- Alsop, G.I., and Holdsworth, R.E., 2004, Shear zone folds: Records of flow perturbation or structural inheritance?, in Alsop, G.I., et al., eds., *Flow Processes in Faults and Shear Zones: Geological Society [London] Special Publication 224*, p. 177–199, <https://doi.org/10.1144/GSL.SP.2004.224.01.12>.
- Alsop, G.I., and Holdsworth, R.E., 2006, Sheath folds as discriminators of bulk strain type: *Journal of*

- Structural Geology, v. 28, p. 1588–1606, <https://doi.org/10.1016/j.jsg.2006.05.005>.
- Bonamici, C.E., Tikoff, B., and Goodwin, L.B., 2011, Anatomy of a 10 km scale sheath fold, Mount Hay ridge, Arunta Region, central Australia: The structural record of deep crustal flow: *Tectonics*, v. 30, TC6015, <https://doi.org/10.1029/2011TC002873>.
- Carreras, J., Druguet, E., and Griera, A., 2005, Shear zone-related folds: *Journal of Structural Geology*, v. 27, p. 1229–1251, <https://doi.org/10.1016/j.jsg.2004.08.004>.
- Chardon, D., Gapais, D., and Cagnard, F., 2009, Flow of ultra-hot orogens: A view from the Precambrian, clues for the Phanerozoic: *Tectonophysics*, v. 477, p. 105–118, <https://doi.org/10.1016/j.tecto.2009.03.008>.
- Cobbold, P.R., and Quinquis, H., 1980, Development of sheath folds in shear regimes: *Journal of Structural Geology*, v. 2, p. 119–126, [https://doi.org/10.1016/0191-8141\(80\)90041-3](https://doi.org/10.1016/0191-8141(80)90041-3).
- Cornish, S., and Searle, M., 2017, 3D geometry and kinematic evolution of the Wadi Mayh sheath fold, Oman, using detailed mapping from high-resolution photography: *Journal of Structural Geology*, v. 101, p. 26–42, <https://doi.org/10.1016/j.jsg.2017.06.009>.
- Dell'Ertolè, D., and Schellart, W.P., 2013, The development of sheath folds in viscously stratified materials in simple shear conditions: An analogue approach: *Journal of Structural Geology*, v. 56, p. 129–141, <https://doi.org/10.1016/j.jsg.2013.09.002>.
- Hanmer, S., and Greene, D.C., 2002, A modern structural regime in the Paleoproterozoic (~3.64 Ga): Isua Greenstone Belt, southern West Greenland: *Tectonophysics*, v. 346, p. 201–222, [https://doi.org/10.1016/S0040-1951\(02\)00029-X](https://doi.org/10.1016/S0040-1951(02)00029-X).
- Huang, B., Kusky, T., Wang, L., Polat, A., Fu, D., Windley, B., Deng, H., and Wang, J.P., 2019, Structural relationships and kinematics of the Neoproterozoic Dengfeng forearc and accretionary complexes, southern North China craton: *Geological Society of America Bulletin*, v. 131, p. 966–996, <https://doi.org/10.1130/B31938.1>.
- Huang, B., Kusky, T.M., Johnson, T.E., Wilde, S.A., Wang, L., Polat, A., and Fu, D., 2020, Paired metamorphism in the Neoproterozoic: A record of accretionary-to-collisional orogenesis in the North China Craton: *Earth and Planetary Science Letters*, v. 543, 116355, <https://doi.org/10.1016/j.epsl.2020.116355>.
- Korenaga, J., 2021, Hadean geodynamics and the nature of early continental crust: *Precambrian Research*, v. 359, 106178, <https://doi.org/10.1016/j.precamres.2021.106178>.
- Kusky, T.M., et al., 2016, Insights into the tectonic evolution of the North China Craton through comparative tectonic analysis: A record of outward growth of Precambrian continents: *Earth-Science Reviews*, v. 162, p. 387–432, <https://doi.org/10.1016/j.earscirev.2016.09.002>.
- Kusky, T.M., Windley, B.F., and Polat, A., 2018, Geological evidence for the operation of plate tectonics throughout the Archean: Records from Archean paleo-plate boundaries: *Journal of Earth Science*, v. 29, p. 1291–1303, <https://doi.org/10.1007/s12583-018-0999-6>.
- Kusky, T.M., et al., 2020, Mélanges through time: Life cycle of the world's largest Archean mélange compared with Mesozoic and Paleozoic subduction-accretion-collision mélanges: *Earth-Science Reviews*, v. 209, 103303, <https://doi.org/10.1016/j.earscirev.2020.103303>.
- Kusky, T., Wang, L., Robinson, P.T., Huang, Y., Wirth, R., Ning, W.B., Zhong, Y.T., and Polat, A., 2021a, Ultra-high pressure inclusion in Archean ophiolitic podiform chromitite in mélange block suggests deep subduction on early Earth: *Precambrian Research*, v. 362, 106318, <https://doi.org/10.1016/j.precamres.2021.106318>.
- Kusky, T., Windley, B.F., Polat, A., Wang, L., Ning, W.B., and Zhong, Y.T., 2021b, Archean dome-and-basin style structures form during growth of intraoceanic and continental margin arcs and their death by slab failure and collision: *Earth-Science Reviews*, v. 220, 103725, <https://doi.org/10.1016/j.earscirev.2021.103725>.
- Lacassin, R., and Mattauer, M., 1985, Kilometre-scale sheath fold at Mattmark and implications for transport direction in the Alps: *Nature*, v. 315, p. 739–742, <https://doi.org/10.1038/315739a0>.
- Lenardic, A., 2018, The diversity of tectonic modes and thoughts about transitions between them: *Philosophical Transactions of the Royal Society of London: Series A, Mathematical, Physical and Engineering Sciences*, v. 376, 20170416, <https://doi.org/10.1098/rsta.2017.0416>.
- Maino, M., Bonini, L., Dallagiovanna, G., and Seno, S., 2015, Large sheath folds in the Briançonnais of the Ligurian Alps reconstructed by analysis of minor structures and stratigraphic mapping: *Journal of Maps*, v. 11, p. 157–167, <https://doi.org/10.1080/17445647.2014.959568>.
- Maino, M., Adamuszek, M., Schenker, F.L., Seno, S., and Dabrowski, M., 2021, Sheath fold development around deformable inclusions: Integration of field-analysis (Cima Lunga unit, Central Alps) and 3D numerical models: *Journal of Structural Geology*, v. 144, 104255, <https://doi.org/10.1016/j.jsg.2020.104255>.
- Mudruk, S.V., Balagansky, V.V., Gorbunov, I.A., and Raevsky, A.B., 2013, Alpine-type tectonics in the Paleoproterozoic Lapland-Kola orogen: *Geotectonics*, v. 47, p. 251–265, <https://doi.org/10.1134/S0016852113040055>.
- National Academies of Sciences, Engineering, and Medicine, 2020, A Vision for NSF Earth Sciences 2020–2030: *Earth in Time*: Washington, D.C., National Academies Press, 304 p., <https://doi.org/10.17226/25761>.
- Nutman, A.P., Bennett, V.C., Friend, C.R.L., and Yi, K., 2020, Eoarchean contrasting ultra-high-pressure to low-pressure metamorphisms (<250 to >1000°C/GPa) explained by tectonic plate convergence in deep time: *Precambrian Research*, v. 344, 105770, <https://doi.org/10.1016/j.precamres.2020.105770>.
- Percival, J.A., Skulski, T., Sanborn-Barrie, M., Stott, G.M., Leclair, A.D., Corkery, M.T., and Boily, M., 2012, Geology and tectonic evolution of the Superior Province, Canada, in Percival, J.A., et al., eds., *Tectonic Styles in Canada: The LITHOPROBE Perspective*: Geological Association of Canada Special Paper 49, p. 321–378.
- Searle, M.P., and Alsop, G.I., 2007, Eye-to-eye with a mega-sheath fold: A case study from Wadi Mayh, northern Oman Mountains: *Geology*, v. 35, p. 1043–1046, <https://doi.org/10.1130/G23884A.1>.
- Seno, S., Dallagiovanna, G., and Vanossi, M., 1998, From finite strain data to strain history: A model for a sector of the Ligurian Alps, Italy: *Journal of Structural Geology*, v. 20, p. 573–585, [https://doi.org/10.1016/S0191-8141\(97\)00104-1](https://doi.org/10.1016/S0191-8141(97)00104-1).
- Sun, G.Z., Liu, S.W., Cawood, P., Tang, M., van Hunen, J., Gao, L., Hu, Y.L., and Hu, F.Y., 2021, Thermal state and evolving geodynamic regimes of the Meso- to Neoproterozoic North China Craton: *Nature Communications*, v. 12, 3888, <https://doi.org/10.1038/s41467-021-24139-z>.
- Wang, J.P., Kusky, T., Wang, L., Polat, A., Deng, H., Wang, C., and Wang, S.J., 2017, Structural relationships along a Neoproterozoic arc-continent collision zone, North China craton: *Geological Society of America Bulletin*, v. 129, p. 59–75, <https://doi.org/10.1130/B31479.1>.
- Wang, J.P., Li, X.W., Ning, W.B., Kusky, T., Wang, L., Polat, A., and Deng, H., 2019, Geology of a Neoproterozoic suture: Evidence from the Zunhua ophiolitic mélange of the Eastern Hebei Province, North China Craton: *Geological Society of America Bulletin*, v. 131, p. 1943–1964, <https://doi.org/10.1130/B35138.1>.
- Wang, J.P., Kusky, T., Polat, A., Wang, L., Deng, H., and Wang, S.J., 2013, A late Archean tectonic mélange in the Central Orogenic Belt, North China Craton: *Tectonophysics*, v. 608, p. 929–946, <https://doi.org/10.1016/j.tecto.2013.07.025>.
- Warren, C.J., Parrish, R.R., Searle, M.P., and Waters, D.J., 2003, U-Pb age of high-pressure metamorphism beneath the Semail Ophiolite, Oman: *Geology*, v. 31, p. 889–892, <https://doi.org/10.1130/G19666.1>.
- Weller, O.M., and St-Onge, M.R., 2017, Record of modern-style plate tectonics in the Palaeoproterozoic Trans-Hudson orogen: *Nature Geoscience*, v. 10, p. 305–311, <https://doi.org/10.1038/ngeo2904>.
- Windley, B.F., Kusky, T., and Polat, A., 2021, Onset of plate tectonics by the early Archean: *Precambrian Research*, v. 352, 105980, <https://doi.org/10.1016/j.precamres.2020.105980>.
- Zhong, Y.T., Kusky, T., Wang, L., Polat, A., Liu, X.Y., Peng, Y.Y., Luan, Z.K., Wang, C.H., Wang, J.P., and Deng, H., 2021, Alpine-style nappes thrust over ancient North China continental margin demonstrate large Archean horizontal plate motions: *Nature Communications*, v. 12, 6172, <https://doi.org/10.1038/s41467-021-26474-7>.

Printed in USA